Mechanical properties of the human Achilles tendon, in vivo

M. Kongsgaard [a,*], C.H. Nielsen [a], S. Hegnsvad [a], P. Aagaard [b], S.P. Magnusson [a,c]

[a] Institute of Sports Medicine, Dept. Othopedic Surgery M, Bispebjerg Hospital and Center for Healthy Aging, Faculty of Health Sciences, University of Copenhagen, Denmark
[b] Institute of Sports Exercise and Clinical Biomechanics, University of Southern Denmark, Odense, Denmark
[c] Department of Physiotherapy, Bispebjerg Hospital, Copenhagen, Denmark

ABSTRACT

Background: Ultrasonography has been widely applied for in vivo measurements of tendon mechanical properties. Assessments of human Achilles tendon mechanical properties have received great interest. Achilles tendon injuries predominantly occur in the tendon region between the Achilles-soleus myotendinous junction and Achilles-calcaneus osteotendinous junction i.e. in the free Achilles tendon. However, there has been no adequate ultrasound based method for quantifying the mechanical properties of the free human Achilles tendon. This study aimed to: 1) examine the mechanical properties of the free human Achilles tendon in vivo by the use of ultrasonography and 2) assess the between-day reproducibility of these measurements.
Methods: Ten male subjects had the Achilles tendon moment arm length, Achilles tendon cross sectional area and free Achilles tendon length determined. All subjects performed isometric plantarflexion ramp contractions to assess between-day reproducibility on two separate days. Simultaneous ultrasonography based measurements of Achilles-soleus myotendinous junction and Achilles-calcaneus osteotendinous junction displacement together with Achilles tendon force estimates yielded free Achilles tendon mechanical properties.
Findings: Free Achilles tendon maximal force, deformation and stiffness were 1924 (SD 229) N, 2.2 (SD 0.6) mm and 2622 (SD 534) N/mm on day 1. For between-day reproducibility there were no significant differences between days for free Achilles tendon mechanical properties. The between-day correlation coefficient and typical error percent were 0.81 and 5.3% for maximal Achilles tendon force, 0.85 and 11.8% for maximal Achilles tendon deformation and 0.84 and 8.8% for Achilles tendon stiffness respectively. Last, osteotendinous junction proximal displacement on average contributed with 71 (SD 12) % of proximal myotendinous junction displacement.
Interpretation: This study, for the first time, presents an ultrasonography based in vivo method for measurement of free AT mechanical properties. The method is applicable for evaluation of free human Achilles tendon mechanical properties in relation to training, injury and rehabilitation.

© 2011 Elsevier Ltd. All rights reserved.

1. Introduction

B-mode ultrasonography has become highly popular for the in vivo measurements of human tendon mechanical properties since the technique is quite inexpensive, non-invasive and easy to use. Especially the assessment of Achilles tendon (AT) mechanical properties has received much attention because of its importance for normal human locomotion (Komi et al., 1987, 1992; Scott and Winter, 1990) and because AT injuries are rather prevalent and difficult to treat (Clement et al., 1984; Cook et al., 2002; Longo et al., 2009; Sandmeier and Renstrom, 1997). However, due to the length of the free human AT, which extends from the calcaneus insertion to the most distal part of the soleus (Calleja and Connell, 2010), B-mode ultrasonography based estimations of AT mechanical properties have been limited. Presently, measurements of the proximal displacement

of the distal myotendinous junction of the medial gastrocnemius in relation to an external marker are typically used to give an estimate of AT mechanics (Arampatzis et al., 2007, 2010; Arya and Kulig, 2010; Bryant et al., 2008; Child et al., 2010; Csapo et al., 2010; Hansen et al., 2003; Lichtwark and Wilson, 2005; Magnusson et al., 2001; Muraoka et al., 2005; Rosager et al., 2002). Inherently this method has some methodological problems (Maganaris, 2005). First, the measured deformation will be a product of the individual elongation of both the free AT and the more proximal aponeurosis structures. Since strain behavior and mechanical properties of the free tendon and aponeurosis structures may differ considerably (Lieber et al., 1991; Magnusson et al., 2003), and since some regions of the aponeurosis may even shorten during muscle contractions (Finni et al., 2003; Kinugasa et al., 2008), this may complicate the interpretation and applicability of such data. Secondly, the displacement of the distal myotendinous junction of the medial gastrocnemius is measured in relation to an external marker (Arampatzis et al., 2007, 2010; Arya and Kulig, 2010; Child et al., 2010; Csapo et al., 2010; Hansen et al., 2003; Lichtwark and Wilson, 2005; Magnusson et al., 2001; Muraoka

et al., 2005; Rosager et al., 2002), and thus any vertical marker displacement will lead to a faulty estimation of the tendon–aponeurosis deformation (Maganaris, 2005). Thirdly, only the displacement of the proximal end of the tendon is measured, which probably yields a significant overestimation of strain (Shin et al., 2008). Ideal assessment of free AT elongation, defined as the actual displacement between the calcaneus and the soleus-AT myotendinous junction, does not include deformation of any aponeurosis structures, and possible displacement of the calcaneus is accounted for, thus rendering the use of an external marker unnecessary. Evaluation of free human AT mechanical properties has previously been performed by tantalum bead implantation in conjunction with Roentgen stereophotogrammetric analysis (Schepull et al., 2007, 2010) and by the used of advanced magnetic resonance imaging techniques (velocity-encoded, phase-contrast MRI) (Kinugasa et al., 2010; Shin et al., 2008). However, the aforementioned techniques have limited applicability since they are invasive and/or quite technically advanced, respectively. To the best of our knowledge, ultrasonography based in vivo assessments of the human AT mechanical properties based on free AT elongation have not previously been performed. However, recent technological advances have made the production of longer ultrasound heads, and therefore also a complete visualization of the entire free Achilles tendon, possible. Therefore, the purposes of the present study were: 1) to examine the mechanical properties of the free human AT, in vivo, by the use of B-mode ultrasonography and 2) to assess the between-day reproducibility of these measurements.

2. Methods

2.1. Subjects

Ten male subjects with a mean age, body weight and height of 30.6 (SD 6.1) yr, 78.9 (SD 6.4) kg and 183 (SD 5) cm volunteered for the study. All subjects were recreational athletes who engaged in various physical activities. No subjects had a history of previous or present AT or lower limb/foot injuries.

2.2. Design

On day 1 all subjects attended measurements of AT moment arm length, free AT length, AT cross sectional area (CSA) and free AT mechanical properties as described in details later. In all subjects, the foot/leg of the preferred leg was used for assessments. To assess the between-day reproducibility of the measurement of the free AT mechanical properties, all subjects attended re-measurements one week following the first test-day. On day 2 the Achilles tendon structural properties were not assessed since reproducibility of these measures were not a part of the purpose of this study. Instead, the Achilles tendon structural properties obtained at day one were used for the calculation of tendon stress, strain and modulus for day 2 assessments. All subjects were investigated at the same time of day on day 1 and day 2.

2.3. Experimental set-up

2.3.1. AT moment arm

As previously described in detail (Scholz et al., 2008; Zhao et al., 2008) the AT moment arm was measured as the perpendicular distance from the center of rotation (axis trough the inferior tip of medial and lateral malleoli) (Scholz et al., 2008) to the AT line of action (LoA). In brief, the inferior tip of the medial and lateral malleolus was marked, and two lines (D1 and D2, Fig. 1) extending from each malleoli to the posterior aspect of the AT were drawn on the skin. Subsequently, the foot was photographed in the lateral and medial sagital planes (Panasonic Lumix DMC-TZ5, Digital Camera) (Fig. 1). The length of lines D1 and D2 were then measured using ImageJ
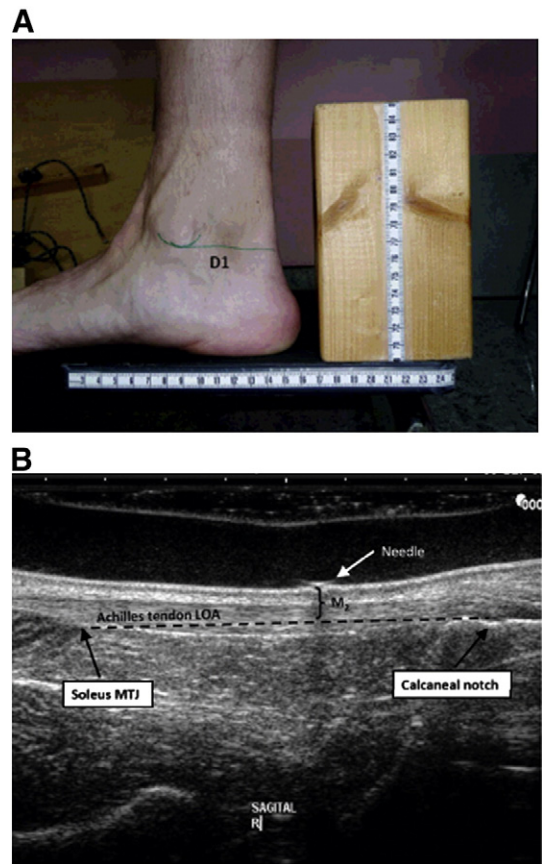

Fig. 1. Achilles tendon (AT) length and moment arm measurements. (A) Two horizontal lines (D1 and D2) were drawn from the inferior tip of the medial and lateral malleoli respectively, to the posterior aspect of the AT. The mean distance of D1 and D2 was calculated as M_1. (B) A Hitachi EUB-6500 ultrasound scanner equipped with a 10 MHz, 100 mm long transducer was used to visualize the intersection of lines D1 and D2 (steel needle) and the AT line of action (LoA). From this image the distance from the D1–D2 intersection to the AT LoA was measured as M_2. The AT moment arm was calculated as $M_A = M_1 - M_2$. The AT length was measured as the shortest vertical distance between the soleus MTJ and the calcaneal notch.

version 1.42 software (http://rsbweb.nih.gov/ij/download.html), and the mean of these two measurements (M_1) was calculated.

Thereafter, a Hitachi EUB-6500 ultrasound scanner (Hitachi Medical Corporation, Tokyo, Japan) equipped with a 10 MHz, 100 mm long, linear array B-mode transducer (Hitachi, Model: EUP-L53L) fitted with a water pad, was used to produce a sagittal plane ultrasonography (US) image of the AT. In this image the intersection of lines D1 and D2 was indicated with a steel needle (Fig. 1) and the perpendicular distance (M_2) from the D1–D2 intersection to the AT LoA was measured using ImageJ software (Fig. 1). The AT moment arm was calculated as: $M_A = M_1 - M_2$ (Zhao et al., 2008). Pilot trials (see later discussion) indicated that the degree of joint rotation, with the current set-up, was negligible and therefore deemed to not significantly affect moment arm length during contraction. Thus, no attempts were made to correct for changes in moment arm during contraction.

2.3.2. AT structural properties

On day 1 subjects were seated with a 90° hip and knee angle and a neutral ankle joint angle (0° dorsiflexion). A sagittal US image of the AT was obtained and the length of the free AT was measured using ImageJ software as the shortest vertical distance between the calcaneal notch and the soleus-Achilles myotendinous junction (MTJ) (Fig. 1). Following this, the location of Achilles-calcaneal OTJ and the soleus-Achilles MTJ were marked on the skin. Three points indicating 25% (proximal), 50% (mid) and 75% (distal) of free AT length was

marked on the skin. From each of these points (proximal, mid and distal) three transversal perpendicular ultrasonography images were obtained for a total of 9 images. From each image the AT CSA was outlined and measured using ImageJ software. The average CSA value of the three scans from each point was used as the AT CSA at that point.

2.3.3. Free AT mechanical properties

Following shaving and cleansing of the skin of the preferred leg, bipolar EMG surface electrodes (Medicotest, Type QN-10A, Ølstykke, Denmark) were placed over the mid-part of the tibialis anterior muscle and the lower medial part of the soleus muscle with a 2 cm inter-electrode distance. A reference electrode was placed on the bony medial aspect of the shin. To precondition the tendon, subjects biked for 5 min with a self-chosen effort on a stationary bike.

Subjects were then seated in a custom made rigid bench with hips and knees in 90° of flexion and the foot in neutral position (0° dorsiflexion) (Fig. 2). The foot was tightly secured on the footplate, with the rotational axis of the foot and footplate in line with each other. The footplate was connected to a strain gauge (Inline Force Sensor, Noraxon Inc., USA) through a vertical rigid steel rod. An iron cross-bar was positioned tightly just behind the lateral femur condyle so that minimal hip, knee or ankle joint movement occurred during isometric contractions.

The subjects performed two 5-s maximal isometric dorsi-flexion efforts with a 2-min rest period to assess the magnitude of antagonist muscle co-activation during the ramped isometric plantar-flexion efforts (Bojsen-Moller et al., 2004) Assuming a linear relationship between EMG amplitude and muscle tension, these data were used to correct for antagonist coactivation during the ramp contractions (Bojsen-Moller et al., 2004). Thereafter, the ultrasound transducer was positioned on the skin (sagittal plane) such that both the AT MTJ and OTJ were clearly visible within the image. Then, subjects performed four 10-s isometric maximal effort ramp contractions (Bojsen-Moller et al., 2004), each separated by a 2-min rest period. During the ramps, ultrasound S-VHS video images were sampled at 25 Hz using frame-by-frame capturing software (Matrox Morphis
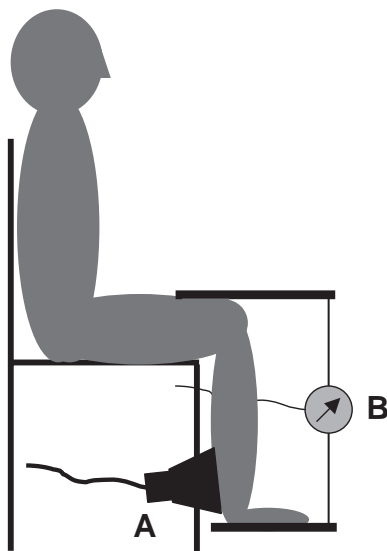
Dual frame grabber and Matrox Imaging Library software, Matrox Electronic Systems Ltd., Montreal, Canada). Free AT deformation (L) during the ramp contractions was defined as the change in linear distance in the sagittal plane between the AT MTJ and OTJ. A custom made frame-by-frame tracking software, using a pyramidal implementation of the Lukas–Kanade optical flow estimation, was used to assess the tendon deformation from the ultrasound videos. The accuracy and reproducibility of this tracking software have previously been assessed (Magnusson et al., 2003).

Force and EMG activity were synchronously sampled at 1500 Hz using a wireless transmitter (8-channel, TeleMyo 2400T G2, Telemetry System, Noraxon Inc., USA) and a PC-Interface receiver (TeleMyo PC-Interface receiver, Noraxon Inc., USA). A trigger signal (Pulse generator, PG 58AA, Gould[Advance], Essex, England) initiated EMG and force sampling while producing a visual marker on the ultrasound video, thus allowing for subsequent synchronization of all recorded data. Pilot trials ($n = 6$) with an electrical goniometer (Inline mechanical goniometer, Noraxon Inc., USA) positioned over the medial aspect of the ankle joint revealed that ankle joint movement during maximal isometric plantar efforts ranged 0.6–1.4° (mean 1.1 (SD 0.4) °) of plantar-flexion.

For all raw data signals (EMG, force) every third data point was extracted to yield an effective sampling frequency of 500 Hz. Subsequently, EMG signals were linearly detrended and highpass filtered using a 4th order Butterworth zerolag highpass filter with a 2 Hz cutoff frequency, followed by full wave rectification and smoothing using a moving RMS filter with a 200-ms time constant (100 data points). All force signals were filtered using a 4th order Butterworth zerolag low pass filter with an 8 Hz cutoff frequency.

Total Achilles tendon force was determined by dividing the externally measured plantarflexor torque (calculated as load cell force multiplied by the external moment arm length) by the internal moment arm obtained in individually in each subject from US measurements as described earlier. To correct for the force contributed by coactivation of the antagonist dorsiflexor muscles (represented by TA) during the graded plantar flexor ramp contraction, the antagonist dorsiflexor torque was estimated from the relationship between TA EMG activity and recorded torque during seperate dorsiflexor MVC contractions, assuming a linear relation between the recorded EMG amplitude and muscle torque (Bojsen-Moller et al., 2004). Subsequently, during analysis of the plantarflexor ramps the estimated antagonist dorsiflexor torque was added to the measured plantarflexor torque prior to calculating the net Achilles tendon force.

3. Data reduction and statistical analysis

The two isometric plantarflexion ramp contractions, obtained on the same day for a given subject, that yielded the greatest AT force were used for further analysis. By combining synchronized AT force (F) and free AT deformation (L) values, a force–deformation relationship was obtained for each of these two ramps (Fig. 3). The load-displacement data were fitted with a 2nd or 3rd order polynomial fit, which in all cases exceeded $R^2 = 0.95$. Tendon stress and strain were calculated by dividing tendon force and deformation by the smallest free AT CSA and the length of the free AT, respectively. Tendon stiffness ($\Delta F/\Delta L$) and modulus (Δstress/Δstrain) were calculated in the final 20% of the force–deformation and stress–strain curves, respectively, assuming a linear relationship between force and elongation in this region (Kubo et al., 2000; Magnusson et al., 2001). It was not the purpose of this study to investigate the reproducibility of ultrasonography based assessment of the tendon structural properties. Paired student's t-test (systematic error), Pearson correlation coefficient (strength of relationship) and typical error percent for duplicate measures of AT maximal force, AT maximal deformation and AT stiffness obtained at day 1 and day 2 for a given subject were used to analyze for reproducibility (Hopkins, 2000). The latter was
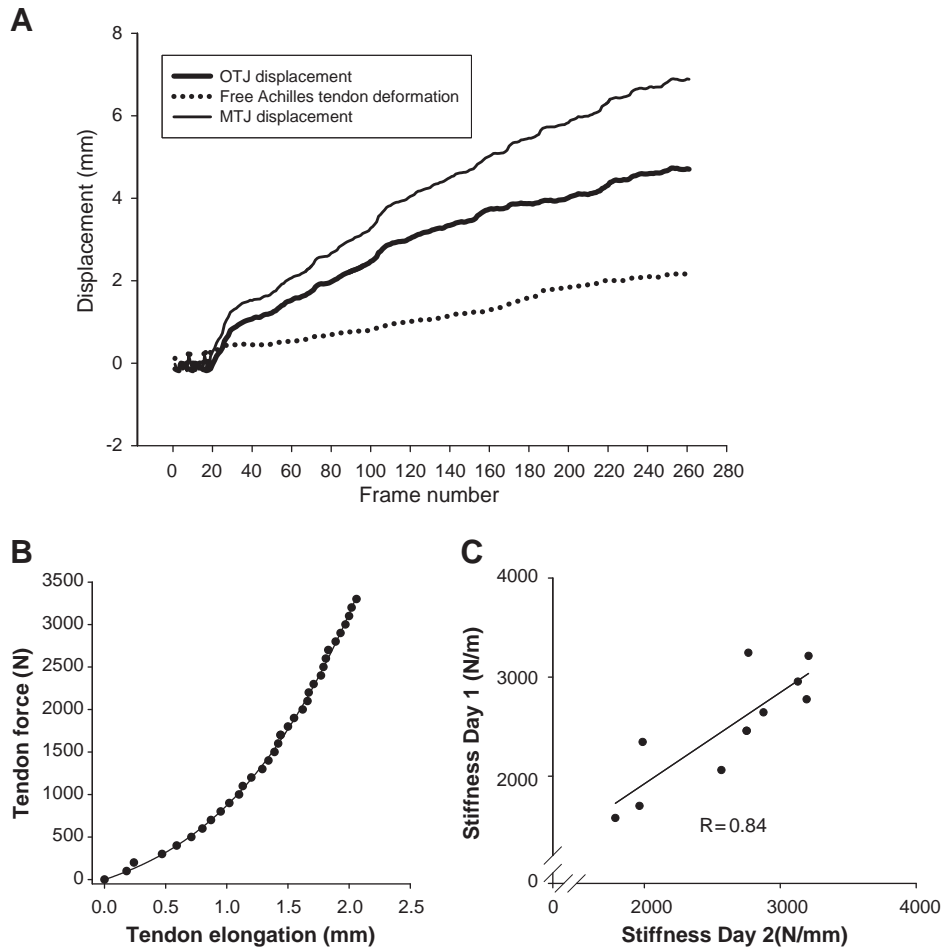

Fig. 2. Illustration of the custom made rigid bench. Subjects were seated with hips and knees in 90° of flexion and the foot in neutral position (0° dorsiflexion). The ultrasound transducer (A) was positioned such that both the AT MTJ and OTJ were clearly visible within the image. The foot was tightly secured on the footplate and the plate adjusted such that the rotational axis of the plate corresponded to that of the ankle joint. The footplate was attached to a strain gauge (B) through a vertical rigid steel rod. An iron cross-bar firmly positioned across the thigh just behind the lateral femur condyle minimized joint movement during contractions.

Fig. 3. (A) The osteotendinous junction (OTJ) displacement, myotendinous junction (MTJ) displacement and the resultant free Achilles tendon deformation during a ramp contraction for one subject. (B) The resulting Achilles tendon force–deformation relationship that was fitted with a polynomial fit. (C) Individual day 1 and day 2 stiffness values plotted against each other (R = Pearson correlation coefficient).

calculated as $SD_{diff}/\sqrt{2}*100\%$. An alpha level of <0.05 was considered as significant. All data are reported as means (SD).

4. Results

Mean results for AT structural properties are reported in Table 1 and mean values for free Achilles tendon mechanical properties and reproducibility assessment is reported in Table 2. On day 1 a mean AT max force of 1924 (SD 229) N produced a mean maximal tendon deformation of 2.2 (SD 0.6) mm, a mean maximal stress of 29 (SD 3) MPa and a mean maximal tendon strain of 4.2 (SD 1.1) %. On day 2 a mean AT max force of 2011 (SD 667) N was obtained, which yielded a mean AT max deformation of 2.4 (SD 0.7) mm, a mean AT max stress of 31 (SD 4) MPa and a mean AT max strain of 4.5 (SD 1.4) %. AT stiffness and modulus were 2622 (SD 534) N/mm and 2.0 (SD 0.4) GPa, respectively, on day 1 and 2497 (SD 584) N/mm and 1.9 (SD 0.5) GPa respectively on day 2. For between-day reproducibility there

were no significant differences between days for maximal AT force, maximal AT deformation, maximal AT stress, maximal AT strain, AT stiffness or AT modulus. The correlation coefficient and typical error percent were 0.81 and 5.63% for maximal AT force, 0.85 and 11.8% for maximal AT deformation and 0.84 and 8.8% for AT stiffness respectively (Fig. 3).

Last, all isometric contractions produced both proximal AT MTJ and OTJ displacement (Fig. 3). The proximal displacement of the AT OTJ during the isometric ramp contractions average 4.9 (SD 0.8) mm whereas the proximal displacement of the AT MTJ junction average 7.1 (SD 0.9) mm (pooled day 1 and day 2 ramps). Consequently, proximal OTJ displacement on average contributed with 71 (SD 12) % of the total proximal MTJ displacement.

5. Discussion

The main finding of this study was that the mechanical properties of the free human Achilles tendon could be determined in a reproducible manner in vivo by the use of B-mode ultrasonography from day to day. Also, it was observed that a considerable proximal displacement of the calcaneus took place during the plantarflexion ramp contractions despite near isometric conditions externally. In fact, approximately 71% of the proximal displacement of the Achilles-soleous MTJ originated from a proximal displacement of the Achilles-calcaneal OTJ, and it is therefore absolutely necessary to account for this when assessing the mechanical properties of the AT.

Table 1
Achilles tendon structural properties.

AT moment arm (mm)	AT CSA prox. (mm²)	AT CSA mid (mm²)	AT CSA dist. (mm²)	AT length (mm)
43 (SD 6)	74 (SD 9)	67 (SD 8)	81 (SD 11)	55 (SD 9)

AT = Achilles tendon, CSA = cross sectional area, prox.= proximal, dist.=distal. Values are mean (SD).

Table 2
Free Achilles tendon mechanical properties and reproducibility hereof.

	AT max. force (N)	AT max. def. (mm)	AT max. stress (MPa)	AT max. strain (%)	AT stiffness (N/mm)	AT modulus (GPa)
Day 1	1924 (SD 229)	2.2 (SD 0.6)	29 (SD 3)	4.2 (SD 1.1)	2622 (SD 534)	2.0 (SD 0.4)
Day 2	2011 (SD 667)	2.4 (SD 0.7)	31 (SD 4)	4.5 (SD 1.4)	2497 (SD 584)	1.9 (SD 0.5)

AT = Achilles tendon, def. = deformation, Max. = Maximal. Values are mean (SD).

The use of ultrasonography based estimations of AT mechanical properties is widespread, but has so far been methodologically challenging. Previous methods have estimated Achilles tendon mechanical properties from measurements of distal medial gastrocnemius MTJ displacement in relation to an external marker. This method, however, has a number of possible errors and inherent limitations (Magnusson et al., 2003; Shin et al., 2008). First, the measured deformation will be a product of the individual elongation of both the free AT and the more proximal tendon–aponeurosis structures, and the two components cannot be distinguished. Given that the free AT is the most common region of tendon ruptures and tendinopathy, and that mechanical properties and mechanical behavior of the free tendon and the more distal tendon–aponeurosis structures may differ considerably during loading (Finni et al., 2003; Kinugasa et al., 2008, 2010; Maganaris and Paul, 2000; Magnusson et al., 2003; Zuurbier et al., 1994), the interpretation and applicability of such data are compromised. In contrast to previously applied ultrasonography based methods for assessment of AT mechanical properties, the methodological approach applied in this present study does not include a mechanical contribution of the proximal tendon–aponeurosis structures and does therefore allow measurement of the isolated free Achilles tendon mechanical properties. The ability to discriminate between the mechanical behavior of the free Achilles tendon and the more proximal aponeurosis structures is underlined by recent, and very interesting, findings showing that some regions of the soleus and gastrochnemius aponeuroses *shorten* under load (Finni et al., 2003; Kinugasa et al., 2008). Last, the presently proposed methodology allows for assessment of changes in AT mechanical properties following suturing and rehabilitation of AT ruptures. Previously this has been addressed by measuring displacement of invasively implanted tantalum beads with the use of dual-beam X-Ray (Schepull et al., 2007, 2010). Thus, the present applied method will in the future allow us to investigate the effect of training, load modification and injury upon the vulnerable free human Achilles tendon. Moreover, by using an ultrasound transducer with a broad field of view (i.e. 100 mm) the present methodology permitted the evaluation of free Achilles tendon mechanical properties without the influence of measurement errors related to skin and marker displacement, vertical transducer movement, and unaccounted calcaneus displacement (Magnusson et al., 2001; Shin et al., 2008). There are however also limitations to the present method. The displacement/strain values, and therefore also tendon mechanical properties, obtained with the present method, only represent values for a selected part of the Achilles tendon cross sectional area. The present method measure the proximal displacement of the most distal part of the Achilles-soleus myotendinous junction. However, not all muscle fibers of the soleus attach to this point of the tendon. Therefore, different magnitudes of strain/displacement might occur within the Achilles cross section area and there might be regional differences in mechanical properties within the tendon that the method cannot account for. However, the present method cannot account for the possibility of intra cross sectional variations in strain behavior and mechanical properties.

In this study we observed a considerable proximal displacement of the calcaneus during the plantarflexion ramp contractions despite that external ankle joint movement was negligible. Pilot trials prior to this study revealed that maximal ankle joint rotation during

the intended isometric plantarflexion ramp contractions was less than 2°. Prior studies using similar conditions have reported ankle joint rotation correction factors in the range of 0.52–0.65 mm displacement/° for the Achilles tendon (Bojsen-Moller et al., 2004; Magnusson et al., 2003). Thus, from this study it can be concluded that a considerable displacement of the calcaneus takes place during isometric plantarflexion ramp contractions despite a lack of externally measured joint rotation. The specific cause of this displacement cannot be established by this study. However, most likely the soleus contraction and subsequent traction of the AT causes an isolated proximal displacement of the calcaneus(Maganaris, 2005). Additionally, it is possible that a distal movement of the transducer takes place thereby generation a relative proximal displacement of the calcaneus within the ultrasonography image. Thus, in agreement with the recent findings by Shin et al. (Shin et al., 2008) and Maganaris et al. (Maganaris, 2005) this study shows that omitting measurement of distal AT end movement will cause a considerable underestimation of AT mechanical properties.

In this study, free AT stiffness and modulus was 2622 (SD 534) N/mm and 2.0 (SD 0.4) GPa respectively. These values are considerably higher than those previously reported by studies applying ultrasonograhy based estimations of Achilles tendon and aponeurosis mechanical properties (Arampatzis et al., 2010; Arya and Kulig, 2010; Csapo et al., 2010; Foure et al., 2010; Hansen et al., 2003; Maganaris and Paul, 2002; Magnusson et al., 2003; Muraoka et al., 2005; Rosager et al., 2002). On the other hand they are very much in line with findings from in vitro examination of human AT mechanical properties (Ker et al., 1988) and with values obtained for the human patellar tendon (Carroll et al., 2008; Hansen et al., 2006; Kongsgaard et al., 2007). Most likely, the somewhat higher values of stiffness and modulus found in this study can be explained by the fact that the presently applied methodology, in contrast to previous studies, account for the tilt generated displacement of the calcaneus. Omitting calcaneus displacement will lead to overestimation of AT strain and thus an underestimation of stiffness and modulus. In support of this assumption, Shin et al. have recently shown by the use of velocity-encoded phase-contrast MRI that proximal calcaneus movement during a near-isometric plantarflexion accounted for 52% of the total tendon displacement (Shin et al., 2008). Additionally, methodological differences related to force estimation, assessment of tendon structural properties, inclusion of aponeurosis structures and differences in correctional factors (i.e. joint rotation and antagonist co-contraction) may contribute to differences in reported mechanical properties.

6. Conclusion

The present study presented an in vivo ultrasonography based method for assessing mechanical properties of the free human Achilles tendon. The method was found to be reproducible and showed that a significant proximal displacement of the calcaneus occurs during maximal ramped near-isometric plantarflexion. The between-day correlation coefficient and typical error percent were 0.84 and 8.8% for AT stiffness respectively. Thus we conclude that the method can be applied to assess and monitor the mechanical properties of the free human Achilles tendon.

Conflict of interest

Acknowledgements

References

Arampatzis, A., Karamanidis, K., Morey-Klapsing, G., De, M.G., Stafilidis, S., 2007. Mechanical properties of the triceps surae tendon and aponeurosis in relation to intensity of sport activity. J. Biomech. 40, 1946–1952.

Arampatzis, A., Peper, A., Bierbaum, S., Albracht, K., 2010. Plasticity of human Achilles tendon mechanical and morphological properties in response to cyclic strain. J. Biomech.. doi:10.1016/j.jbiomech.2010.08.014 Epub.

Arya, S., Kulig, K., 2010. Tendinopathy alters mechanical and material properties of the Achilles tendon. J. Appl. Physiol 108, 670–675.

Bojsen-Moller, J., Hansen, P., Aagaard, P., Svantesson, U., Kjaer, M., Magnusson, S.P., 2004. Differential displacement of the human soleus and medial gastrocnemius aponeuroses during isometric plantar flexor contractions in vivo. J. Appl. Physiol 97, 1908–1914.

Bryant, A.L., Clark, R.A., Bartold, S., Murphy, A., Bennell, K.L., Hohmann, E., et al., 2008. Effects of estrogen on the mechanical behaviour of the human Achilles tendon in vivo. J. Appl. Physiol 105, 1035–1043.

Calleja, M., Connell, D.A., 2010. The Achilles tendon. Semin. Musculoskelet. Radiol. 14, 307–322.

Carroll, C.C., Dickinson, J.M., Haus, J.M., Lee, G.A., Hollon, C.J., Aagaard, P., et al., 2008. The influence of aging on the in vivo properties of human patellar tendon. J. Appl. Physiol 105, 1907–1915.

Child, S., Bryant, A.L., Clark, R.A., Crossley, K.M., 2010. Mechanical properties of the achilles tendon aponeurosis are altered in athletes with achilles tendinopathy. Am. J. Sports Med. 38, 1885–1893.

Clement, D.B., Taunton, J.E., Smart, G.W., 1984. Achilles tendinitis and peritendinitis: etiology and treatment. Am. J. Sports Med. 12, 179–184.

Cook, J.L., Khan, K.M., Purdam, C., 2002. Achilles tendinopathy. Man. Ther. 7, 121–130.

Csapo, R., Maganaris, C.N., Seynnes, O.R., Narici, M.V., 2010. On muscle, tendon and high heels. J. Exp. Biol. 213, 2582–2588.

Finni, T., Hodgson, J.A., Lai, A.M., Edgerton, V.R., Sinha, S., 2003. Nonuniform strain of human soleus aponeurosis–tendon complex during submaximal voluntary contractions in vivo. J. Appl. Physiol 95, 829–837.

Foure, A., Nordez, A., Cornu, C., 2010. Plyometric training effects on Achilles tendon stiffness and dissipative properties. J. Appl. Physiol 109, 849–854.

Hansen, P., Aagaard, P., Kjaer, M., Larsson, B., Magnusson, S.P., 2003. The effect of habitual running on human Achilles tendon load-deformation properties and cross-sectional area. J. Appl. Physiol 95, 2375–2380.

Hansen, P., Bojsen-Moller, J., Aagaard, P., Kjaer, M., Magnusson, S.P., 2006. Mechanical properties of the human patellar tendon, in vivo. Clin. Biomech. 21, 54–58.

Hopkins, W.G., 2000. Measures of reliability in sports medicine and science. Sports Med. 30, 1–15.

Ker, R.F., Alexander, R.M., Bennett, M.B., 1988. Why are mammalian tendons so thick? J Zool. Lond. 216, 309–324.

Kinugasa, R., Shin, D., Yamauchi, J., Mishra, C., Hodgson, J.A., Edgerton, V.R., et al., 2008. Phase-contrast MRI reveals mechanical behavior of superficial and deep aponeuroses in human medial gastrocnemius during isometric contraction. J. Appl. Physiol 105, 1312–1320.

Kinugasa, R., Hodgson, J.A., Edgerton, V.R., Shin, D.D., Sinha, S., 2010. Reduction in tendon elasticity from unloading is unrelated to its hypertrophy. J. Appl. Physiol 109, 870–877.

Komi, P.V., Salonen, M., Jarvinen, M., Kokko, O., 1987. In vivo registration of Achilles tendon forces in man. I. Methodological development. Int. J. Sports Med. 8 (Suppl 1), 3–8.

Komi, P.V., Fukashiro, S., Jarvinen, M., 1992. Biomechanical loading of Achilles tendon during normal locomotion. Clin. Sports Med 11, 521–531.

Kongsgaard, M., Reitelseder, S., Pedersen, T.G., Holm, L., Aagaard, P., Kjaer, M., et al., 2007. Region specific patellar tendon hypertrophy in humans following resistance training. Acta Physiol 191, 111–121.

Kubo, K., Kanehisa, H., Kawakami, Y., Fukunaga, T., 2000. Elastic properties of muscle-tendon complex in long-distance runners. Eur. J. Appl. Physiol 81, 181–187.

Lichtwark, G.A., Wilson, A.M., 2005. In vivo mechanical properties of the human Achilles tendon during one-legged hopping. J. Exp. Biol. 208, 4715–4725.

Lieber, R.L., Leonard, M.E., Brown, C.G., Trestik, C.L., 1991. Frog semitendinosis tendon load–strain and stress–strain properties during passive loading. Am. J. Physiol 261, C86–C92.

Longo, U.G., Ronga, M., Maffulli, N., 2009. Acute ruptures of the Achilles tendon. Sports Med Arthrosc. 17, 127–138.

Maganaris, C.N., 2005. Validity of procedures involved in ultrasound-based measurement of human plantarflexor tendon elongation on contraction. J. Biomech. 38, 9–13.

Maganaris, C.N., Paul, J.P., 2000. In vivo human tendinous tissue stretch upon maximum muscle force generation. J. Biomech. 33, 1453–1459.

Maganaris, C.N., Paul, J.P., 2002. Tensile properties of the in vivo human gastrocnemius tendon. J. Biomech. 35, 1639–1646.

Magnusson, S.P., Aagaard, P., Dyhre-Poulsen, P., Kjaer, M., 2001. Load-displacement properties of the human triceps surae aponeurosis in vivo. J. Physiol 531, 277–288.

Magnusson, S.P., Hansen, P., Aagaard, P., Brond, J., Dyhre-Poulsen, P., Bojsen-Moller, J., et al., 2003. Differential strain patterns of the human gastrocnemius aponeurosis and free tendon, in vivo. Acta Physiol Scand. 177, 185–195.

Muraoka, T., Muramatsu, T., Fukunaga, T., Kanehisa, H., 2005. Elastic properties of human Achilles tendon are correlated to muscle strength. J. Appl. Physiol 99, 665–669.

Rosager, S., Aagaard, P., Dyhre-Poulsen, P., Neergaard, K., Kjaer, M., Magnusson, S.P., 2002. Load-displacement properties of the human triceps surae aponeurosis and tendon in runners and non-runners. Scand. J. Med. Sci. Sports 12, 90–98.

Sandmeier, R., Renstrom, P.A., 1997. Diagnosis and treatment of chronic tendon disorders in sports. Scand. J. Med. Sci. Sports 7, 96–106.

Schepull, T., Kvist, J., Andersson, C., Aspenberg, P., 2007. Mechanical properties during healing of Achilles tendon ruptures to predict final outcome. A pilot Roentgen stereophotogrammetric analysis in 10 patients. BMC Musculoskelet. Disord. 8, 116.

Schepull, T., Kvist, J., Aspenberg, P., 2010. Early E-modulus of healing Achilles tendons correlates with late function: similar results with or without surgery. Scand. J. Med. Sci. Sports. doi:10.1111/j.1600-0838.2010.01154.x E-pub.

Scholz, M.N., Bobbert, M.F., van Soest, A.J., Clark, J.R., van Heerden, J., 2008. Running biomechanics: shorter heels, better economy. J. Exp. Biol. 211, 3266–3271.

Scott, S.H., Winter, D.A., 1990. Internal forces of chronic running injury sites. Med. Sci. Sports Exerc. 22, 357–369.

Shin, D., Finni, T., Ahn, S., Hodgson, J.A., Lee, H.D., Edgerton, V.R., et al., 2008. Effect of chronic unloading and rehabilitation on human Achilles tendon properties: a velocity-encoded phase-contrast MRI study. J. Appl. Physiol 105, 1179–1186.

Zhao, H., Ren, Y., Wu, Y.N., Liu, S.Q., Zhang, L.Q., 2008. Ultrasonic evaluations of Achilles tendon mechanical properties post stroke. J. Appl. Physiol 106, 843–849.

Zuurbier, C.J., Everard, A.J., van der Wees, P., Huijing, P.A., 1994. Length–force characteristics of the aponeurosis in the passive and active muscle condition and in the isolated condition. J. Biomech. 27, 445–453.